Efficient, Automated Cycle-Slip Correction Of Dual-Frequency Kinematic GPS Data

Sunil B. Bisnath

Geodetic Research Laboratory, Department of Geodesy and Geomatics Engineering, University of New Brunswick, Fredericton, New Brunswick, Canada.

BIOGRAPHY

Sunil Bisnath received a B.Sc. (Hons.) in 1993 and an M.Sc. in 1995 in Surveying Science from the University of Toronto. He is currently a Ph.D. candidate in the Department of Geodesy and Geomatics Engineering at the University of New Brunswick, where he is investigating the use of GPS for precise low-earth-orbiter tracking. This research is being performed under the supervision of Professor Richard Langley at the department's Geodetic Research Laboratory.

ABSTRACT

In order to attain high precision positioning and navigation results with GPS, cycle slips must be correctly repaired at the data preprocessing stage. A slip of only a few cycles can bias measurements enough to make centimetre-level positioning or navigation difficult. Over the past decade a number of methods have been developed to detect and repair cycle slips. The majority of approaches involve forming cycle-slip-sensitive linear combinations of the available observables. Algorithms have been designed to detect, determine, and repair these cycle slips by fitting functions to the linear combinations and observing differences between the functions and the data combinations. These methods invariably require user intervention for problematic cycle slips in portions of data, tuning of input parameters to data, or introduction of additional carrier-phase ambiguity-resolution parameters in the main data processing where pre-processing cycle-slip determination has failed.

A method has been developed from various existing techniques, that provides fully automatic cycle-slip correction at the data preprocessing stage. The algorithms utilise two dual frequency, double-difference carrier phase and pseudorange geometry-free linear combinations. These combinations are filtered to allow for high-resolution cycle-slip detection, and are then compared with least-squares-fitted Chebyshev polynomials for cycle-slip determination. Results indicate that single-cycle slips can be reliably detected for receivers in varied environments, and that these slips can be repaired correctly.

INTRODUCTION

The use of GPS for precise static or kinematic positioning requires the use of carrier-phase measurements. Integer ambiguities in the phase data must be removed to utilise the full measurement strength of the phase observable. This consists of initial integer ambiguities and additional integer ambiguities introduced by cycle slips. For long baseline kinematic data processing (*e.g.*, hundreds or thousands of kilometres) estimation of the initial integer ambiguities is a very difficult undertaking. However, the detection and correction of cycle slips is needed if accurate positioning is to be carried out. This task can be quite labour intensive if semi-automated techniques are used, or can produce erroneous results if inappropriate automated techniques are implemented. Slip detection and repair still represents a challenge to carrier phase data processing even after years of research, early on in which it was predicted [Westrop *et al.*, 1989] that cycle slips would in all likelihood not pose a problem in the future due to receiver advances.

This paper addresses the development of a cycle-slip detection and correction technique designed to detect and correct cycle slips in dual-frequency carrier phase data, in a fully automatic manner, utilising carrier phase and pseudorange measurements in a post-processing environment. The prime objective of the work is to correctly detect and repair *all* cycle slips in the data pre-processing (sometimes referred to as the data editing) stage, with straightforward algorithms not dependent on the quality of the input data.

What is a cycle slip? Briefly it is a sudden integer number of cycles jump in the carrier phase observable,

caused by the loss of lock of the receiver phase lock loops [Leick, 1995]. The loss may be due to internal receiver tracking problems or an interruption in the ability of the antenna to receive the satellite signals [Seeber, 1993]. A loss of lock may be shorter than the time interval between two adjacent data collection epochs or as long as the time interval between many epochs, in which case the term data gap may be in order. The process of cycle-slip correction involves detecting the slip, estimating the exact number of L1 and L2 frequency cycles that comprise the slip, and actually correcting the phase measurements by these integer estimates.

For completeness, a short description of the development of strategies for detecting and determining cycle slips over the past fifteen years or so is presented. This is followed by the description of the enhanced detection and correction method. Results of the new technique presented. Finally concluding remarks and proposals for future research are given.

METHODS OF DETECTING AND DETERMINING CYCLE SLIPS

In this section, a general review of detection and determination philosophies is given, with specific methods and equations expanded upon in the later sections. Texts containing detailed discussions of this topic include Hofmann-Wellenhof *et al.* [1997] and Seeber [1993].

For the most part, techniques used in the detection and determination of cycle slips have not changed drastically since the first methods were devised in the early 1980s. The focus has always been on attempting to develop a reliable, somewhat automatic detection and repair procedure. All methods have the common premise that to detect a slip at least one smooth (*i.e.*, low noise) quantity derived from the observations must be tested in some manner for discontinuities that may represent cycle slips [Lichtenegger and Hofmann-Wellenhof, 1990].

The derived quantities usually consist of linear combinations of the undifferenced or double-differenced L1 and L2 carrier-phase and possibly pseudorange observations. Examples of combinations useful for kinematic data are the ionospheric phase delay (a scaled version of which is called the geometry-free phase) [Goad, 1986; Bastos and Landau, 1988, Blewitt, 1990; Gao and Li, 1999], range residual [Bastos and Landau, 1988], and widelane phase minus narrowlane pseudorange [Blewitt, 1990; Han, 1997; Gao and Li, 1999].

Once the time series for the derived quantities have been produced, the cycle-slip detection process (that is, the detection of discontinuities in the time series) can be initiated. Of the various methods available, only four will be discussed here. The most straightforward method is to compute higher order time differences of the time series, which accentuate any discontinuities. This method is used by many static GPS processing packages including the University of New Brunswick's DIPOP (DIfferential POsitioning Program) software [Kleusberg *et al.*, 1993]. The main disadvantages of this method are that data-set-specific tolerance values have to be set (time difference values that are greater than the tolerances indicate the presence of a cycle slip), and geometry-free linear combinations are required for kinematic data. Another method is to fit a low degree polynomial over the time series and conclude that any large (again, determined for the specific data set) discrepancies between the polynomial and the time series represents a cycle slip [Lichtenegger and Hofmann-Wellenhof, 1990]. This method is also hampered by the number and size of slips altering the shape of the fitting polynomial. A popular method, especially for kinematic data processing where such filtering is used in the main processing stage is Kalman filtering (*e.g.*, Bastos and Landau [1988]; Han [1997]). An adjunct to this technique is the use of wavelets rather than Kalman filtering [Collin and Warnant, 1995]. The predicted time series values estimated from the developed dynamic model in the Kalman filter are compared with the actual data time series. Any statistically significant discrepancies are representative of cycle slips. However, filter tuning is required to chose appropriate filter parameters for the data set and unpredictable results can be obtained, at least with undifferenced static data [Blewitt, 1998]. The final method to be discussed was developed by Blewitt [1990] and consists partially of applying a running average filter to a linear combination to improve the estimate of the combination's ambiguity term. Cycle slips are detected by determining if two consecutive unfiltered data points are outside the confidence interval of the running mean. This method and the Kalman filtering approach have the advantage that they use statistical information from the data themselves in the detection process.

After cycle slips have been detected, the actual number of L1 and L2 cycles that comprise each slip must be determined and then the data corrected. The latter is a simple enough task, but the determination can require additional information. If single-frequency linear combinations resulting in integer ambiguity values are used (such as the single-frequency range residual), then the integer number of cycles attributable to the slip can be directly estimated. If a dual-frequency combination is used, then this single combination consists of two unknowns: the slip in L1 and the slip in L2. Therefore a second linear combination is needed to uniquely solve for the individual frequency slips. This can be accomplished by using one of the detection methods on a second linear combination, not to detect a slip, but rather to estimate the inter-frequency slip. With this additional information, the

values of the L1 and L2 cycle slips can be uniquely determined. Various techniques can be used to fix the estimates to integers, ranging from simple rounding to searching for slip pairs that best fit the linear combinations in a least-squares sense. If viable integer combinations cannot be determined, then additional carrier phase ambiguity resolution parameters can be introduced in the main data processing (*e.g*., Kleusberg *et al*. [1993]; Seeber [1993]).

AN AUTOMATIC CYCLE-SLIP CORRECTION TECHNIQUE

The technique presented here represents an evolution, from static to kinematic and from semi-automatic to fully automatic data handling in the DIPOP preprocessors, the original versions of which are described in Kleusberg *et al*. [1993]. After outlier detection and time tag correction, two satellite-receiver, geometry-free linear combinations are formed with the dual-frequency carrier phase and pseudorange measurements, for each baseline double-difference satellite pair. The noisier of the two combinations is filtered and cycle slips are detected on each combination by means of various tests. The filtered combination is also filtered backwards and the data from the two combinations are used in a least-squares, polynomial fitting strategy to estimate the magnitude and sign of the double-difference L1 and L2 cycle slips in the time series. The estimated slips are applied in a correction routine. A second round of identical detection then takes place to verify correct determination. If any residual slips are detected, the determination and correction routines are again initiated.

OBSERVABLE MODELS

The mathematical models for the raw carrier-phase and pseudorange observables are

for the L1 frequency:

$$\begin{aligned}\Phi_1 &= \lambda_1\phi_1 \\ &= \rho + c(dT - dt) + d_{trop} - d_{ion1} + \lambda_1 N_1 + m_1 + \varepsilon_1,\end{aligned} \quad (1)$$

$$P_1 = \rho + c(dT - dt) + d_{trop} + d_{ion1} + M_1 + e_1, \quad (2)$$

and for the L2 frequency:

$$\begin{aligned}\Phi_2 &= \lambda_2\phi_2 \\ &= \rho + c(dT - dt) + d_{trop} - d_{ion2} + \lambda_2 N_2 + m_2 + \varepsilon_2,\end{aligned} \quad (3)$$

$$P_2 = \rho + c(dT - dt) + d_{trop} + d_{ion2} + M_2 + e_2, \quad (4)$$

where Φ_i and P_i are the measured carrier phase and pseudorange (in distance units), respectively; λ_i is the carrier wavelength; ϕ_i is the measured carrier phase (in cycles); ρ is the geometric range from receiver to the GPS satellite; c is the vacuum speed of light; dT and dt are the offsets of the receiver and GPS satellite clocks from GPS Time, respectively; N_i is the number of cycles by which the initial phases are undetermined; d_{ioni} and d_{trop} are the delays due to the ionosphere and the troposphere, respectively; m_i and M_i represent the effect of multipath on the carrier phases and the pseudoranges, respectively; and ε_i and e_i represent the effect of receiver noise on the carrier phases and the pseudoranges, respectively. Satellite and receiver hardware delays and other small effects have been ignored as they have negligible effect on data preprocessing.

By double differencing the observations (that is, at each epoch differencing between receivers followed by differencing between satellites) the clock offsets can be removed and the linear combinations used in detection and determination are closer to zero slope. The latter situation is helpful, since it accentuates the results of the time differences in the detection by reducing (for short- and medium-length baselines) the size of the ionospheric term. However, following the law of error propagation, the random error in each double-difference is approximately double that of the undifferenced data. The double-difference observables are

for the L1 frequency:

$$\begin{aligned}\nabla\Delta\Phi_1 &= \lambda_1\nabla\Delta\phi_1 = \nabla\Delta\rho \\ &+ \nabla\Delta d_{trop} - \nabla\Delta d_{ion1} + \lambda_1\nabla\Delta N_1 + \nabla\Delta m_1 + \nabla\Delta\varepsilon_1,\end{aligned} \quad (5)$$

$$\nabla\Delta P_1 = \nabla\Delta\rho + \nabla\Delta d_{trop} + \nabla\Delta d_{ion1} + \nabla\Delta M_1 + \nabla\Delta e_1, \quad (6)$$

and for the L2 frequency:

$$\begin{aligned}\nabla\Delta\Phi_2 &= \lambda_2\nabla\Delta\phi_2 = \nabla\Delta\rho \\ &+ \nabla\Delta d_{trop} - \nabla\Delta d_{ion2} + \lambda_2\nabla\Delta N_2 + \nabla\Delta m_2 + \nabla\Delta\varepsilon_2,\end{aligned} \quad (7)$$

$$\nabla\Delta P_2 = \nabla\Delta\rho + \nabla\Delta d_{trop} + \nabla\Delta d_{ion2} + \nabla\Delta M_2 + \nabla\Delta e_2, \quad (8)$$

where $\nabla\Delta$ is the double-difference operator.

DETECTION OBSERVABLES

Two detection observables were chosen so as not to contain any component of satellite-receiver range and to minimise measurement noise. Therefore the two linear combinations produce time series which are relatively invariant to collection time, baseline separation, and static or kinematic data collection modes, within the limits of the residual ionosphere, multipath, and receiver noise. The combinations chosen are the geometry-free phase and the widelane phase minus narrowlane pseudorange. The L1 and L2 range residuals were not used, as the

measurement noise terms of these observables are greater than that of the widelane phase minus narrowlane pseudorange combination. Both of the selected combinations have been utilised for cycle-slip detection by Blewitt [1990] for undifferenced static data, and by Gao and McLellan [1996], and Gao and Li [1999] for double-differenced short baseline static and kinematic data.

Geometry-free phase

The first observable is the geometry-free phase linear combination:

$$\begin{aligned}&\lambda_1\nabla\Delta\phi_1-\lambda_2\nabla\Delta\phi_2\\&=\left(\nabla\Delta d_{ion2}-\nabla\Delta d_{ion1}\right)+\left(\lambda_1\nabla\Delta N_1-\lambda_2\nabla\Delta N_2\right)\\&+\left(\nabla\Delta m_1-\nabla\Delta m_2\right)+\left(\nabla\Delta\varepsilon_1-\nabla\Delta\varepsilon_2\right).\end{aligned}\qquad(9)$$

This combination consists of inter-frequency double-difference ionosphere, L1 and L2 double-difference integer ambiguities, inter-frequency double-difference phase multipath, and inter-frequency double-difference receiver phase noise. Han [1997] notes that this combination has no integer ambiguity characteristic, but such a quality is not required for the detection and determination approach which follows, since the individual L1 and L2 cycle slips are isolated in the determination phase. A cycle slip on the next (post slip) epoch of this combination would result in the ambiguities term being replaced with

$$\left[\lambda_1\left(\nabla\Delta N_1+n_1\right)-\lambda_2\left(\nabla\Delta N_2+n_2\right)\right],\qquad(10)$$

where n_1 and n_2 are the double-difference integer cycle-slips (in cycles) on the L1 and L2 frequencies, respectively.

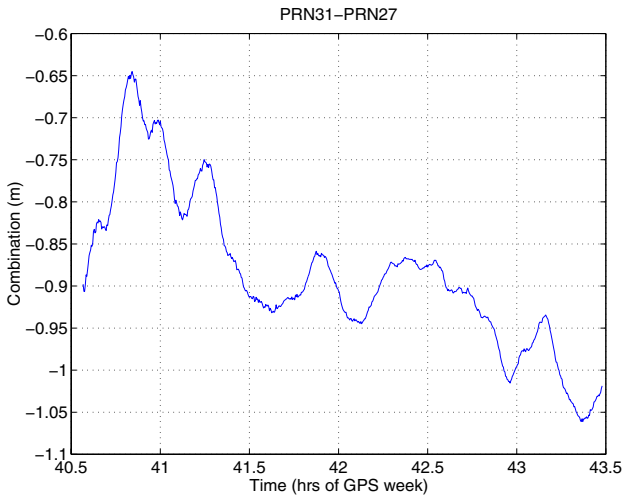

Figure 1: Variation in geometry-free phase combination.

Figure 1 illustrates the behaviour of this observable for a sample of data collected on a static baseline of approximately 200 km. In the figure, the geometry-free phase time series has been differenced from the integer value of its first data point to remove the majority of the observable for which the ambiguity bias is the main constituent. This is done since the variation of the combination is the important aspect in this analysis. The variations are primarily due to the ionospheric term indicated in equation (9), whereas the phase multipath and noise terms have much higher frequencies and lower amplitudes.

Widelane phase minus narrowlane pseudorange

The second observable is the widelane phase minus narrowlane pseudorange linear combination (*e.g.*, Blewitt [1990]; Gao and Li [1999]):

$$\begin{aligned}&\lambda_4\left(\nabla\Delta\phi_1-\nabla\Delta\phi_2\right)-\lambda_5\left(\frac{\nabla\Delta P_1}{\lambda_1}+\frac{\nabla\Delta P_2}{\lambda_2}\right)\\&=\lambda_4\left(\nabla\Delta N_1-\nabla\Delta N_2\right)\\&+\lambda_4\left(\frac{\nabla\Delta m_1}{\lambda_1}-\frac{\nabla\Delta m_2}{\lambda_2}\right)-\lambda_5\left(\frac{\nabla\Delta M_1}{\lambda_1}+\frac{\nabla\Delta M_2}{\lambda_2}\right)\\&+\lambda_4\left(\frac{\nabla\Delta\varepsilon_1}{\lambda_1}-\frac{\nabla\Delta\varepsilon_2}{\lambda_2}\right)-\lambda_5\left(\frac{\nabla\Delta e_1}{\lambda_1}+\frac{\nabla\Delta e_2}{\lambda_2}\right),\end{aligned}\qquad(11)$$

where

$$\lambda_4=\left(\lambda_1^{-1}-\lambda_2^{-1}\right)^{-1}\approx 86.2\text{cm},\qquad(12)$$

usually referred to as the widelane wavelength and

$$\lambda_5=\left(\lambda_1^{-1}+\lambda_2^{-1}\right)^{-1}\approx 10.7\text{cm},\qquad(13)$$

usually referred to as the narrowlane wavelength.

This combination consists of the widelane ambiguity, a residual multipath term, and a residual receiver noise term. Not directly apparent from this formulation, the ionospheric terms cancel since

$$d_{ion1}=\frac{\lambda_1^2}{\lambda_2^2-\lambda_1^2}I\qquad(14)$$

and

$$d_{ion2}=\frac{\lambda_2^2}{\lambda_2^2-\lambda_1^2}I,\qquad(15)$$

where I is the so-called ionospheric delay parameter.

Since the multipath and noise terms of the pseudorange measurements are much larger than those of the carrier phase measurement, the fluctuations in this combination are mainly due to pseudorange multipath and pseudorange measurement noise. The former of these error terms can cause quasi-sinusoidal variations of many metres. A cycle slip on the next (post slip) epoch of this combination would result in the ambiguities term being replaced with

$$\lambda_4\left[\left(\nabla\Delta N_1 + n_1\right) - \left(\nabla\Delta N_2 + n_2\right)\right]. \qquad (16)$$

The noise of this observable makes high resolution cycle-slip detection unlikely. However, Blewitt [1990] proposed a simple running average filter to make this observable more useful. This strategy is quite intuitive, since over time one would expect the residual multipath and noise terms to average down to near constant values. The filter is an expanding-memory, low-pass filter whose output is identical to the recursive mean:

$$\bar{x}_t = \bar{x}_{t-1} + \frac{1}{t}\left(x_t - \bar{x}_{t-1}\right), \qquad (17)$$

where x is the observation, $\bar{x}$ is the mean of x, and t and t-1 represent the present and previous epoch counts, respectively.

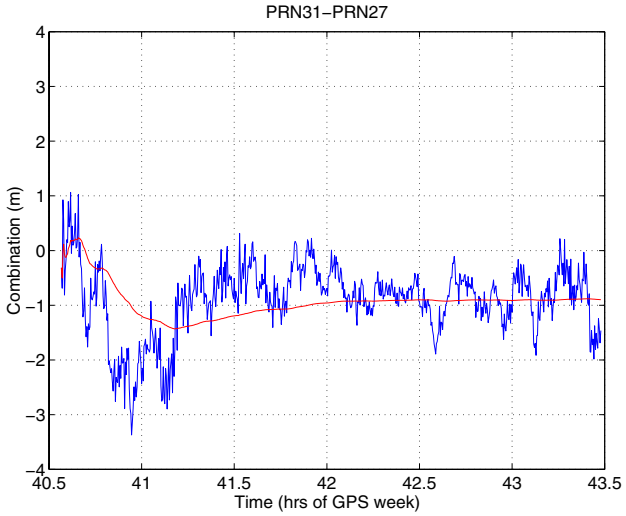

Figure 2: Variation in widelane phase minus narrowlane pseudorange combination. The smooth line shows the running-average filtered values.

Figure 2 depicts this combination for the same data set used in Figure 1. The noise level is substantially higher than for the first combination, but this is tempered with the filtering. The running-average filtered results do not follow the raw data as well as, for example, a moving-average filter, especially due to the large amounts of multipath at the start of the time series. But as long as there are no cycle slips, the running average is a better estimate of the ambiguity bias given these large errors.

DETECTION TESTS

Two different cycle-slip detection tests are performed on each time series of the created combinations. The geometry-free phase combination is first tested, since it has the lower noise.

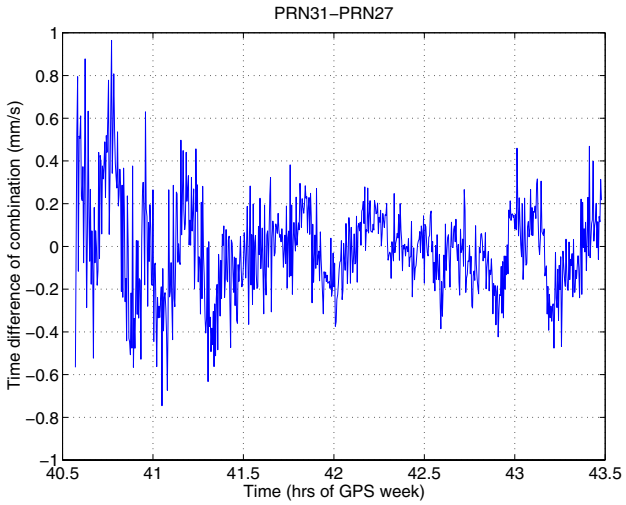

Figure 3: Time difference of geometry-free combination.

The first test investigates the variation of the time-normalised, between-epoch time difference of the geometry-free combination. Figure 3 illustrates this quantity with the data from Figure 1. The principle used here is that a discontinuity in a time series is more pronounced in the time differences of that series, since time differencing is analogous to high-pass filtering [Hofmann-Wellenhof *et al.*, 1997]. From past experience with DIPOP [Kleusberg *et al.*, 1993], a set of four time differences are compared. The median time difference is differenced from the time difference value being tested. The median rather than the mean is used here, as it was found that the former is more robust. For example, even a severe gradient in the rate of change of the ionospheric term will be almost completely removed in the second time differencing. The absolute value of this difference leaves a very small component of the ionospheric, multipath and noise terms, and an estimate of the cycle slip, if any, on this combination. Since a significant amount of spatial and temporal correlation exists in the three problematic terms, this differencing of differences method is quiet robust. The resulting value is differenced from a slip tolerance. In some software, (*e.g.*, Kleusberg *et al.* [1993]), this tolerance must be selected on a per data set basis. This human interaction has been removed in the

new approach by computing the time difference of the smallest type of cycle slip that can consistently be observed with this combination (from equation (10)), *e.g.*,:

$$n_1 = 5,\ n_2 = 4 \Rightarrow \left|\lambda_1 n_1 - \lambda_2 n_2\right| \approx 2.5\,\text{cm}. \qquad (18)$$

More will be said about this slip pairing and the choice of this pairing in the next section.

If a slip is detected, then the second test is carried out. This test takes advantage of a property of time differencing, which is illustrated in Figure 4: a discontinuity at one epoch will appear as two discontinuities adjacent in time.

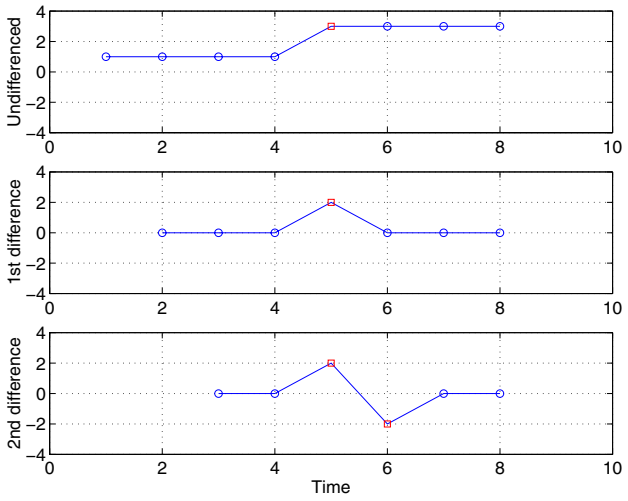

Figure 4: The effect of time differencing given a discontinuity.

For the widelane phase minus narrowlane pseudorange combination, a different approach is used due to the high noise level of the combination. A testing scheme modelled after Blewitt's [1990] technique for undifferenced static data is used. The double-differenced measurements are filtered and the unfiltered data points are compared with ±4σ of the filtered mean.

The recursive standard deviation is computed via Blewitt [1990]

$$\sigma_t^2 = \sigma_{t-1}^2 + \frac{1}{t}\left[(x_t - \bar{x}_{t-1})^2 - \sigma_{t-1}^2\right], \qquad (19)$$

where σ is the biased sample standard deviation and the other variables are as stated in (17). The choice of the *a priori* variance value is not critical, as the recursive algorithm quickly determines variance values which are representative of the data set being processed.

The meaning of this test is that any value outside the expected ambiguity estimate (the running average confidence interval) represents a possible cycle slip. If unfiltered data from previous and subsequent epochs lie outside or within one cycle, respectively, of such a data point, then a slip is declared. If the one-sigma standard deviation of the observations leading up to the potential slip is greater than one widelane cycle an integer is multiplied to the widelane cycle tolerance. This is done so that slips the size of which are below the noise level of the observations are not detected as they may produce type two errors. One method of reducing the need for this second test could be to use a moving average and associated moving standard deviation. While the moving average would not be as good an estimate of the ambiguity bias, the moving standard deviation would better tolerate the effects of pseudorange multipath than the running standard deviation. Another option could be to utilise the receiver signal-to-noise values as an indicator of the combination noise.

An example of this testing is given in Figure 5. The unfiltered data are the same as in Figure 2, and the ±4σ confidence intervals computed from equation (19) have been added.

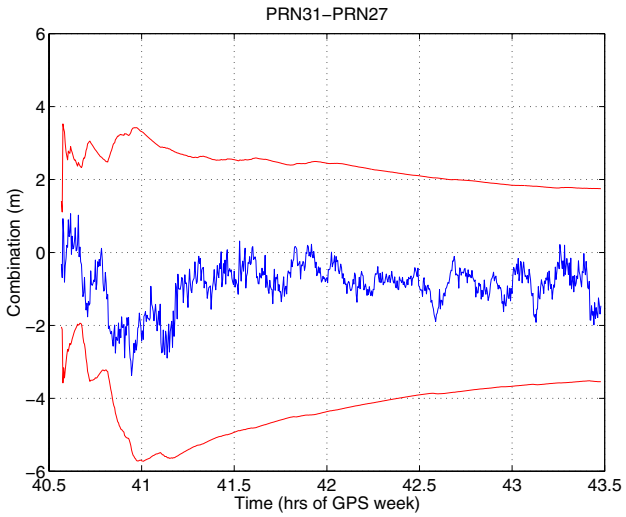

Figure 5: Variations in widelane phase minus narrowlane pseudorange combination with associated ±4σ confidence intervals.

DETECTION INSENSITIVITY

Analysing equations (10) and (16) individually, there are many combinations of cycle slips (n_1 and n_2) which could be missed by the detection algorithms. However as stated by Gao and McLellan [1996], the presented two tiered approach greatly reduces the number of slip pairs which both combinations are insensitive to. Table 1 lists all of these pairs where the slip on the geometry-free combination is less than or equal to one L1 cycle and the

slip on the widelane phase minus narrowlane pseudorange is less than or equal to three widelane cycles. From experience, the geometry-free combination can be used to consistently detect cycle slips as small as a few centimetres, so only the combinations in bold italics are of great concern. These situations have been previously identified by Gao and McLellan [1996], and represent the rationale for the slip tolerance set in the geometry-free phase detection tests. These slip pairs will be discussed further in the testing sections.

From the discussion of the detection test and Table 1, it can be seen that most cycle slips will be detected with the use of the geometry-free combination. And that the widelane phase minus narrowlane pseudorange is used to detect rare types of slips and allow for, along with the geometry-free combination, the determination of the individual double-differenced L1 and L2 frequency cycle-slip estimates.

n_1	n_2	$n_1\lambda_1$-$n_2\lambda_2$ (cm)	$(n_1$-$n_2)\lambda_4$ (cm)
1	1	-5.4	0
2	1	13.6	86.2
2	2	-10.8	0
3	2	8.3	86.2
3	3	-16.2	0
4	***3***	***2.9***	***86.2***
5	***4***	***-2.5***	***86.2***
6	5	-7.9	86.2
7	5	11.1	172.4
7	6	-13.3	86.2
8	6	5.7	172.4
8	7	-18.7	86.2
9	***7***	***0.3***	***172.4***
10	8	-5.1	172.4
11	9	-10.5	172.4
12	10	-15.8	172.4

Table 1: Combination-insensitive cycle-slip pairings.

DETERMINATION

In order to precisely estimate the double-difference cycle slips in the given combinations, the geometry-free phase and widelane phase minus narrowlane pseudorange time series for each double-difference pair are integrated in a Chebyshev polynomial, least-squares fitting scheme.

To utilise the widelane phase minus narrowlane pseudorange combination, the forward and backward runs of the filter are combined to optimally smooth the time series. Following Gelb [1974], the optimal smoothed estimate (unbiased and of minimum variance) is

$$\begin{aligned} \hat{x}_S(t) &= C_S\left[C_F^{-1}\hat{x}_F(t) + C_B^{-1}\hat{x}_B(t)\right], \\ C_S &= \left(C_F^{-1} + C_B^{-1}\right)^{-1}, \end{aligned} \tag{20}$$

where the subscripts F, B, and S indicate forward filter, backward filter, and smoother, respectively; $\hat{x}$ is the linear combination estimate; and C is the covariance matrix. The covariances for the forward and backward filter are estimated from equation (19).

With noisier data it was observed that the smoothing produced roughness at either end of the time series and on either side of detected cycle slips (the so-called "bow-tie" effect). This could cause errors in the slip estimation. To compensate for this, testing was carried out using only data from the forward filter before a cycle slip and data from the backward filter after the slip.

The next step is the polynomial fitting. Chebyshev polynomial fitting was chosen for DIPOP [Kleusberg *et al.*, 1993] since it nearly completely minimises the maximum residuals in the fit, making it a very robust technique. The Chebyshev polynomials are computed based on normalised time series time:

$$T_k(t) = \cos\left[k\cos^{-1}(t)\right], \tag{21}$$

where $T_k(t)$ is the k^{th} Chebyshev polynomial base function at time t. A linear parametric least-squares fit of the polynomials to each linear data combination is then carried out in order to estimate the Chebyshev polynomial coefficients and more importantly the estimates of the cycle slips in each combination. This is represented by

$$cs(t) + \sum_{k=1}^{n} T_{k-1}(t)C_k = obs(t), \tag{22}$$

where cs is a cycle slip, T is a Chebyshev polynomial term, C is a polynomial coefficient, and obs is the time series value. From static DIPOP experience, a polynomial of approximately order 30 is typically used, but it may be appropriate to increase this value by making it a function of the number of epochs of data and the noise level of the widelane phase minus narrowlane pseudorange combination. The combination cycle slips and the polynomial coefficients are estimated in a parametric least-squares adjustment along with the residuals of the least-squares fit. The combination slip estimates, the fit residuals, and the combination observations are then combined in a weighted parametric adjustment to estimate real-valued double-difference L1 and L2 cycle slips. These results are then rounded to obtain integer estimates.

Figure 6 illustrates an example of the determination procedure for a one-cycle cycle slip on L1. The differences in the fitted polynomials before and after the slip for each combination agree well with the theoretical values: 19.0cm for the geometry-free phase and 86.2cm for the widelane phase minus narrowlane pseudorange.

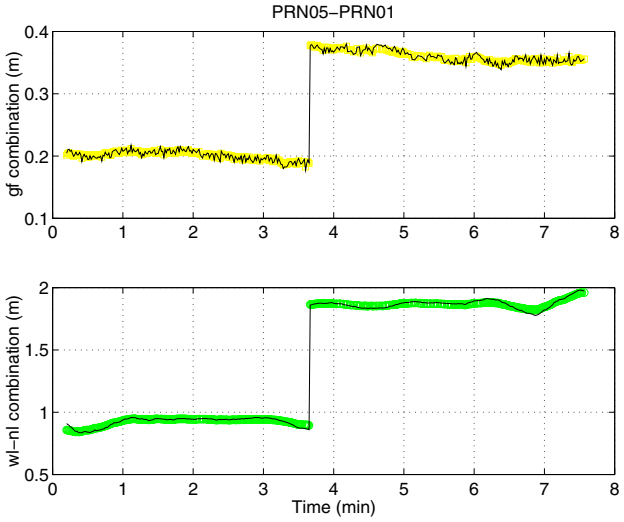

Figure 6: Determination of cycle slip. Thin lines represent combinations and thick, light lines represent fitted polynomials.

STATIC DATA TESTING

In order to test the detection and determination strategy both static and kinematic data were processed. The former is presented here and the latter in the next section.

Static data testing was deemed appropriate, since it allows for a "truth solution" to be determined with a semi-automated technique, using less noisy phase combinations in the cycle-slip correction process. The data set used consists of an approximately 200 km long baseline. The data contain a significant amount of multipath (as seen in Figures 1 and 2), which stem from ground and wall bounce multipath at one of the antenna locations. Such a corrupted data set is representative of an extreme environment and therefore provides a good test of robustness for the described slip correction technique.

The results using this strategy produced the same detected and repaired cycle slips as with the manual processing strategy. The first geometry-free combination test detects a number of cycle slips erroneously, but the second test indicates from differencing that these apparent discontinuities are not cycle slips. The widelane phase minus narrowlane pseudorange test does not incorrectly detect any slips, and the smoothing of these time series allow for precise estimation of the L1 and L2 slips. An example of a detected slip is shown in Figure 7. The slip can be observed at approximately 40.4 hours on this time difference of the geometry-free combination. The slip is equal to two double-difference cycles on L1 and two double-difference cycles on L2, and therefore is not detectable on the widelane phase minus narrowlane pseudorange combination (see Table 1).

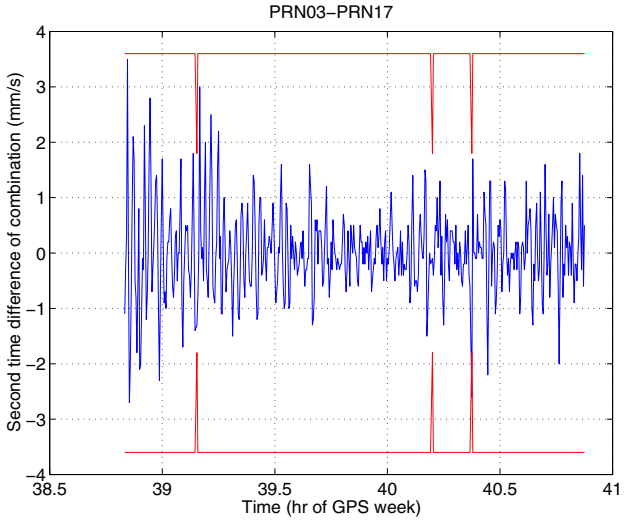

Figure 7: Detected cycle slip in static data using geometry-free phase combination. The almost continuously horizontal lines are the slip tolerances for the first geometry-free phase detection test.

The above detection could be made much more difficult during periods of large ionospheric fluctuations, when the ionospheric term represents the main noise contributor in the geometry-free phase combination. Gao and McLellan [1996] indicated that a few-epoch moving average of the geometry-free phase combination subtracted from the actual combination can greatly reduce the effect of the ionospheric term, as long as the multipath is insignificant. Blewitt [1990] describes avoiding large discontinuities due to the changing ionospheric conditions by using a high data collection rate.

KINEMATIC DATA TESTING

The kinematic tests involve a marine situation, in which the vessel data were collected at an average distance of 40 km from the reference receiver. This data set is representative of typical measurement conditions. The "truth solution" was obtained via a complex Kalman filtering procedure with manual verification. The results using the presented strategy compare favourably with the Kalman filtering results in that both processing techniques produce the same results.

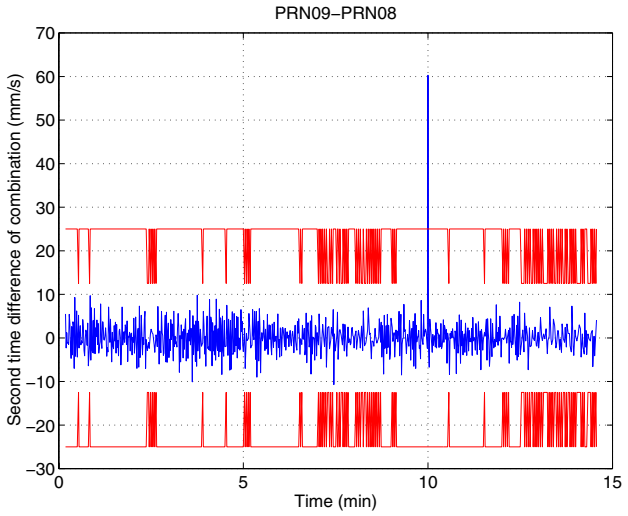

Figure 8: Detected cycle slip in kinematic data using geometry-free phase combination.

Given that Table 1 indicates various problematic cycle-slip pairs, slip pairs of this kind were injected into this kinematic data set to test the technique's sensitivity. The results indicate that, with the tested data set, the most sensitive pairings described in Table 1 can be detected and corrected with this technique. For example, the effect of the pairing $n_1 = 5$, $n_2 = 4$ can be clearly seen in Figure 8 at approximately 10 minutes. The time differencing of the geometry-free combinations greatly accentuates the slip and it can be detected unambiguously.

CONCLUSIONS AND FUTURE RESEARCH

A completely automatic cycle-slip detection, determination, and repair technique has been developed to preprocess dual-frequency, kinematic (and static) GPS data. The individual algorithms stem from research performed by various authors, and combined here in a novel procedure. The technique relies on the detection of cycle slips via two geometry-free linear combinations of the dual-frequency GPS measurements, namely the geometry-free phase and the widelane phase minus narrowlane pseudorange. Slips are detected for each combination via a number of geometric and statistical tests, the results of which when combined represent a high-resolution, yet straightforward method for detecting cycle slips. The determination of detected slips is performed by integrating the two combinations in a Chebyshev polynomial, least-squares fitting scheme.

Results using extremely noisy static and typical kinematic data, with both actual and simulated cycle slips, indicate that the technique is correctly detecting and repairing cycle slips (and only needed marginally increased processing time). Given that data sets vary significantly in the numbers and size of cycle slips and levels of ionospheric delay, multipath and noise, more testing is required in order to further validate the performance of the technique. Possible improvements to the algorithms include the use of a moving standard deviation for detection on the widelane phase minus narrowlane pseudorange, and the use of receiver signal-to-noise values for the noise estimation. Determination may be improved with the use of fitting polynomials better tailored to the data, and the use of other geometry-free combinations.

ACKNOWLEDGEMENTS

The author would like to thank Dr. Richard Langley for his supervision and financial support through the Natural Sciences and Engineering Research Council of Canada and the GEOIDE Network of Centres of Excellence. Also acknowledged are colleagues Dr. Donghyun Kim for processing the kinematic data set from the Canadian Hydrographic Service and the Canadian Coast Guard, and Mr. Paul Collins for processing one static data set which includes data from the United States Continuously Operating Reference Stations (CORS) network.

REFERENCES

Bastos, L. and H. Landau, (1988). "Fixing cycle slips in dual-frequency kinematic GPS-applications using Kalman filtering," *Manuscripta Geodaetica*, Vol. 13, No. 4, pp. 249-256.

Blewitt, G. (1990). "An automatic editing algorithm for GPS data," *Geophysical Research Letters*, Vol. 17, No. 3, pp. 199-202.

Blewitt, G. (1998). "GPS data processing methodology," in *GPS for Geodesy*. 2nd Edition, P.J.G. Teunissen and A. Kleusberg (Eds.), Springer-Verlag, Berlin, 650 pp.

Collin, F. and R. Warnant, (1995). "Application of the wavelet transform for GPS cycle slip correction and comparison with Kalman filter," *Manuscripta Geodaetica*, Vol. 20, No. 3, pp. 161-172.

Gao, Y. and Z. Li, (1999). "Cycle slip detection and ambiguity resolution algorithms for dual-frequency GPS data processing," *Marine Geodesy*, Vol. 22, no. 4, pp. 169-181.

Gao, Y. and J.F. McLellan, (1996). "An analysis of GPS positioning accuracy and reliability with dual-frequency data." *Proceedings of the 9th International Technical Meeting of the Satellite Division of the Institute of Navigation*, Kansas City, Kansas, U.S.A., 17-20 September, 1996, The Institute of Navigation, Alexandria, Virginia, U.S.A., Vol. 1, pp. 945-951.

Gelb, A. (Ed.) (1974). *Applied Optimal Estimation.* The MIT Press, Massachusetts Institute of Technology, Cambridge, 374 pp.

Goad, C. (1986). "Precise positioning with the Global Positioning System," *Proceedings of the Third International Symposium on Inertial Technology for*

Surveying and Geodesy, 16-20 September 1985, Banff, Canada, pp. 745-756.

Han, S. (1997). "*Carrier phase-based long-range GPS kinematic positioning*," UNISURV S-49, School of Geomatic Engineering, The University of New South Wales, 185 pp.

Hofmann-Wellenhof, B., H. Lichtenegger, and J. Collins. (1997). *GPS Theory and Practice.* 4th Edition, Springer-Verlag, Wien, 389 pp.

Kleusberg, A., Y. Georgiadou, F. van den Heuvel, and P. Heroux (1993). "*GPS data preprocessing with DIPOP 3.0*," internal technical memorandum, Department of Surveying Engineering (now Department of Geodesy and Geomatics Engineering), University of New Brunswick, Fredericton, 84 pp.

Leick, A. (1995). *GPS Satellite Surveying.* 2nd Edition, John Wiley and Sons, Inc., New York, 560 pp.

Lichtenegger, H. and B. Hofmann-Wellenhof (1990). "GPS-data preprocessing for cycle-slip detection." *Global Positioning System: an overview*. Y. Bock and N. Leppard (Eds.), International Association of Geodesy Symposia 102, Edinburgh, Scotland, 2-8 August, 1989, pp.57-68.

Seeber, G. (1993). *Satellite Geodesy.* Walter de Gruyter and Co., Berlin, 531 pp.

Westrop, J, M.E. Napier, and V. Ashkenazi (1989). "Cycle slips on the move: detection and elimination." *Proceedings of the 2nd International Technical Meeting of the Satellite Division of the Institute of Navigation*, Colorado Springs, Colorado, U.S.A., 27-29 September, 1989, The Institute of Navigation, Alexandria, Virginia, U.S.A., pp. 31-34.